# Trends and Solar Cycle Effects in Temperature versus Altitude from the Halogen Occultation Experiment for the Mesosphere and Upper Stratosphere

Ellis E. Remsberg[1,*]

1--Science Directorate, NASA Langley Research Center, Hampton, Virginia, USA

*denotes corresponding author (E. E. Remsberg, Science Directorate, 21 Langley Blvd., Mail Stop 401B, NASA Langley Research Center, Hampton, VA 23681-2199. (e-mail: Ellis.E.Remsberg@nasa.gov)).

**Abstract.** Fourteen-year time series of mesospheric and upper stratospheric temperatures from the Halogen Occultation Experiment (HALOE) are analyzed and reported. The data have been binned according to ten-degree wide latitude zones from 40S to 40N and at 10 altitudes from 43 to 80 km—a total of 90 separate time series. Multiple linear regression (MLR) analysis techniques have been applied to those time series. This study focuses on resolving their 11-yr, solar cycle (or SC-like) responses and their linear trend terms. Findings for T(z) from HALOE are compared directly with published results from ground-based Rayleigh lidar and rocketsonde measurements. SC-like responses from HALOE compare well with those from lidar station data at low latitudes. The cooling trends from HALOE also agree reasonably well with those from the lidar data for the concurrent decade. Cooling trends of the lower mesosphere from HALOE are not as large as those from rocketsondes and from lidar station time series of the previous two decades, presumably because the changes in the upper stratospheric ozone were near zero during the HALOE time period and did not affect those trends.

## 1. Background and Objectives

Earth's upper atmosphere has been cooling and its pressure surfaces contracting due to the full radiative effect of the rising greenhouse gas concentrations, particularly of $CO_2$ [*Laštovička et al.*, 2006]. Model predictions are qualitatively consistent with the observed contraction of the thermosphere based on several decades of satellite drag measurements [*Roble and Dickinson,* 1989; *Emmert et al.,* 2004]. *Remsberg* [2008a] also found a long-term cooling on constant pressure surfaces of the upper mesosphere that was somewhat greater than -1.0 K/decade at middle latitudes, based on his analyses of 14-yr (1991-2005) temperature time series from the Halogen Occultation Experiment (HALOE) [*Russell et al.,* 1993] of the Upper Atmosphere Research Satellite (UARS). That rate of cooling for the mesosphere is also roughly consistent with what was predicted [*Roble and Dickinson,* 1989].

In the present paper the temperature trends from the HALOE data are reanalyzed and reported for constant altitudes rather than pressure levels, in order to compare them more directly with some recent published findings from ground-based lidar and microwave measurements for the same time period. Trends in temperature versus altitude (or T(z)) are affected by temperature changes in the underlying atmospheric column, while the results for temperature versus pressure (or T (p)) are based on physical processes at the local pressure level. The concurrent and periodic, 11-yr response in T(z) is resolved, too, and shown to be in-phase with the solar cycle flux at most altitudes. The trends in T(z) from the HALOE data are also contrasted with published results based on lidar and rocket measurements of earlier decades, when decreases in ozone were occurring in the stratosphere and contributing to a further contraction of the atmospheric column from the upper stratosphere to the middle mesosphere.

## 2. Data Analysis Approach

*Remsberg* [2008a, and references therein] concluded that the atmospheric sampling of the HALOE experiment was adequate for resolving the seasonal and longer-period variations in its temperature profiles after they had been bin-averaged within latitude zones. The 95,900 sunrise (SR) plus sunset (SS) scan profiles have good signal-to-noise for the altitude range of this study, and there is a calibration against an exo-atmospheric, Sun-look for each scan [*Russell et al.,* 1993]. Furthermore, no significant trends were found for the HALOE instrument and its 2.8-µm $CO_2$ channel transmission measurements that were used for the retrieval of T(z) above about 38 km [*Gordley et al.,* 2009]. Below that altitude the retrieved HALOE T(z) essentially relies on a tie-on to profiles from the 12Z operational temperature analyses provided to the UARS Project by the NOAA Climate Prediction Center (CPC). A retrieval tie-on was also made to the Mass Spectrometer and Incoherent Scatter (MSIS)-90 empirical atmospheric model above about 85 km. The vertical resolution of the retrieved portion of the HALOE T(z) profile is about 3.5 km or similar to that reported for ground-based lidar profiles.

Time series of bin-averaged profiles were obtained from the SR and then the SS measurements within 10-degree wide latitude zones from 40S to 40N and for 10 altitude levels from 43 to 80 km. A minimum of 5 profiles was required for each bin-averaged point. The seasonal sampling from HALOE was not as good for higher latitudes, so those regions were not evaluated for their temperature trends. The SR and SS data at a latitude and altitude were combined into a single time series after adjusting the SR and SS points for the average difference of their separate time series. The effects of the diurnal temperature tide are accounted for by that adjustment to first order, as shown in *Remsberg* [2007; 2008a]. As an example, Figure 1 presents the adjusted T(z) time series of over 200 points from HALOE for 30N and 75 km. It is realized that the tidal amplitudes also undergo some seasonal variation, especially at low latitudes. Thus, the present approach to a tidal adjustment imparts a small bias to the amplitudes of the seasonal terms for the present analyses, but not to those of the longer period terms.

The oscillating curve in Figure 1 is a multiple linear regression (MLR) model fit to the time series points. The MLR model is composed of constant (Const), annual (AO), semi-annual (SAO), quasi-biennial (QBO) and sub-biennial (IA) terms, an 11-yr or solar cycle-like (SC) term, and a linear trend (Lin) term. The straight line includes the Lin term that has been plotted relative to its value midway between 1991 and 2005. The QBO and IA terms have average periods of 853 days and 640 days, respectively, as determined by Fourier fits to the time series residuals after accounting for the seasonal terms. Amplitudes of those interannual terms in T(z) are very similar to their values for T(p) in *Remsberg* [2008a]. After accounting for the seasonal and interannual terms the time series of the residuals was checked for any remaining periodic structure—an important test for the acceptance of the final MLR model. Proxy terms related to forcings from the eruption of Mt. Pinatubo or the aperiodic El Nino/Southern Oscillation (ENSO) index were not added to the MLR models because the residuals did not show any clearly anomalous features.

The linear trend term from the MLR model of Figure 1 is -2.2 K/decade and is significant at the 99% confidence interval (CI). This trend value is in reasonable accord with other observations, as will be shown in Section 4. The response of temperature to the solar cycle has been evaluated by most researchers by fitting the time series points with a proxy term for the solar flux. Instead, the approach used in this study is to merely fit a sinusoid of 11-yr period and then to check the phase of its maximum to see whether it was within a year or so of solar cycle flux maximum as described in more detail in *Remsberg* [2007]. This alternate approach has been used because there may also be decadal-scale changes in temperature due to dynamical forcings [e.g., *Hampson et al.,* 2005; *Shibata and Kodera*, 2005]. Nevertheless as shown in Section 3, the 11-yr MLR term is in-phase (or very nearly so) for many of the temperature time series. In the case of Figure 1 the amplitude of the 11-yr term is highly significant, and its maxima occur in late January 1992 and 2003 or 1.1 years after the approximate times of the maxima for the solar cycle uv-flux. Some studies are showing that the 11-yr solar cycle response in temperature can be more apparent for a particular season or phase of the QBO cycle [e.g., *Matthes et al.,* 2004]. However, the HALOE dataset provides many fewer points for time series partitioned in those ways, leading to large reductions in the significance of all their MLR terms. The 11-yr and trend terms of the present analyses are representative of the zonal-mean, annual-average temperature distribution from HALOE.

## 3. The 11-yr and SC-like Responses

A total of 90 separate T(z) time series like that of Figure 1 are analyzed in the present study. Their MLR models include both an 11-yr term and a linear trend term. In this section the character and significance of their 11-yr or SC-like terms are considered. Their quality and validity are judged based on the magnitudes and phases of the max minus min responses and for the pattern and continuity of the terms within the altitude/latitude domain. If they are reasonable, then it is likely that the concurrent linear trend terms of Section 4 are meaningful, too.

Figure 2 is the contour plot of the max minus min responses for the 11-yr term. The dark shading denotes those regions having CI greater than 90%; lighter gray shadings have a CI of between 70 and 90%. Figure 3 is the contour plot of the phase of the 11-yr terms. Darker shading denotes those regions where the 11-yr terms have their maximum values within +/-1.5 years of January 1991 and 2002—the approximate midrange time for the maxima of the traditional solar flux proxies. Figure 3 shows that the 11-yr term is very nearly in-phase with solar maxima over most the domain. A notable exception occurs for the region of weak responses of the mid mesosphere at northern hemisphere middle latitudes (Figure 2), just below the altitude region having a larger response. In fact, the largest 11-yr responses occur in the mid and upper mesosphere at middle latitudes, and they are in-phase. However, there is some asymmetry between the southern and northern hemispheres for those responses, quite possibly due to associated differences from effects of decadal-scale, wave forcings.

Figure 4 is the contour plot of the solar-cycle (SC-like) max minus min T(z) values that were obtained by multiplying the 11-yr responses of Figure 2 by the cosine of the ratio of the corresponding phase lead or lag (in years) of Figure 3 to the 11-yr period of the SC. In effect, Figure 4 is the approximate response one would find by performing a regression of the HALOE T(z) time series against a more traditional solar flux proxy. One can directly compare the T(z) results of Figure 4 with the analysis results for time series of the ground-based Rayleigh lidar station measurements. As an example, Table 1 provides the HALOE values at 10N and at 20N along with the lidar results at Gadanki (13.5N) of *Sridharan et al.* [2008] and at Mauna Loa (19.5N) of *Li et al.* [2008], respectively, and for a similar set of years. At both locations there is good agreement for the magnitudes of the SC-like responses from HALOE and lidar. On the other hand, the lidar results at these two latitudes tend to be out-of-phase with the solar cycle in the upper mesosphere, while the HALOE results are less so. It is noted that the lidar results are averages of measurements obtained over several nighttime hours, whereas the HALOE results are strictly from its SR and SS measurements. Perhaps this difference indicates that there is a decadal or solar cycle effect in the tidal forcings at low latitudes, where the tidal amplitudes are large. *Batista et al.* [2008] looked for a solar cycle response in their lidar temperature time series at 23S, but they did not find any significant values for the altitudes of 40 to 60 km. Figure 4 shows that the responses near 23S from HALOE are also no greater than about 0.5 K for those altitudes.

Table 1 also compares the annually-averaged, SC-like response profile from HALOE at 40N with that from the lidar at Haute Provence, France (44N), but based on its longer period of observations from 1979/2001 [*Keckhut et al.,* 2005]. Nevertheless, because the SC forcing is essentially periodic the responses of temperature to it ought to be similar for multiple solar cycles. Responses from those lidar data were reported separately for summer and winter; numerical responses were estimated from their Figure 3 and then averaged for its profile entry in Table 1. The respective HALOE and lidar response profiles agree well in the upper mesosphere and near the stratopause, but not in the middle mesosphere or at 43 km where the HALOE-derived responses are small. It may be that there is more wintertime wave activity affecting the upper stratospheric and mesospheric column over the lidar site than is the case for the zonally-averaged responses of HALOE [*Hampson et al.,* 2006]. More specifically, the lidar temperatures at 44N, 6E are often affected noticeably by sudden stratospheric warming (SSW) events during wintertime, while the HALOE analyses in the 40±5N bin are somewhat equatorward of that latitude and less subject to such local, large-amplitude wave forcings.

Figure 3 shows that the 11-yr responses of the upper stratosphere from HALOE are in-phase with the solar flux at the Equator but are more nearly out-of-phase at middle latitudes. This finding is qualitatively consistent with the weak SC-like responses observed in time series records of lidar and microwave results from 35 to 45 km and for the middle latitude stations of the Network for the Detection of Atmospheric Composition Change (NDACC) [*Steinbrecht et al.,* 2009]. The response of temperature to the solar forcing should be nearly the same for T(z) and T(p), and the contour values and patterns of Figure 4 are very similar to those from HALOE T(p) in *Remsberg* [2008a, Figure 14]. The SC-like, HALOE responses are of order 1 K in the region of the tropical stratopause, and the responses within middle atmosphere, chemistry/climate models are in good agreement with that value [e.g., *Austin et al.,* 2008; *Rind et al.,* 2008; *Tsutsui et al.,* 2009].

**4. Trends in T(z)**

Temperature trends in the mesosphere are a direct measure of the radiative effects from the combined changes in the "greenhouse gas" concentrations, primarily those of $CO_2$ and $O_3$. Figure 5 shows the linear trends for ozone on a pressure surface from HALOE, so that one can know how it was changing for the 1991-2005 period at specific levels of the atmosphere. Those trends are nearly zero through the upper stratosphere and up to at least 0.2 hPa (~60 km). In the middle stratosphere the HALOE ozone trends were still decreasing, as discussed in more detail in *Remsberg* [2008b].

The associated linear trends in T(z) are presented in this section and compared with concurrent findings from station data. Then the HALOE T(z) trends are contrasted with the findings from lidar and rocket station time series data of the preceding decade or two, when the ozone of the upper stratosphere was declining at a rate of about -5 to -7%/decade [*WMO* , 2003]. Keeping in mind that the T(z) trend for a given altitude reflects the effects of the ozone changes within the underlying atmospheric column, it is likely that there was an enhanced rate of cooling in the upper stratosphere and lower mesosphere at that earlier time [*Akmaev et al.,* 2006].

Figure 6 shows the T(z) trends from HALOE in terms of K/decade. In order to be consistent with the convention for the contours of T(p) in *Remsberg* [2008a], the solid contours are the cooling trends, while the dashed contours define the zero and warming trends. The darker shading denotes those regions where the confidence intervals (CI) for the trends are greater than 90%; lighter shading defines regions having CI of between 70 and 90%. One can see that significant cooling was occurring for this period across the region of the mid to lower mesosphere, and that it exhibited good continuity from 40S to 40N. In general, the trends in T(z) are more negative than those for T(p) of *Remsberg* [2008a] because the trends for T(z) represent the effects of the cooling for the underlying atmospheric column. T(z) trends in the upper stratosphere from the HALOE data vary between 0.0 and -0.5 K/decade and are similar to those reported for the 35 to 45 km region from the NDAAC station data [*Steinbrecht, et al.,* 2008].

Table 2 gives HALOE T(z) comparisons with the trend profiles from two low latitude lidar stations—in Brazil [*Batista et al.,* 2008] and in Gadanki [*Sridharan et al.,* 2008]. Cooling trends were found over the altitudes of the upper stratosphere and lower mesosphere from all the datasets, and in most instances the HALOE results agree with the lidar values. For the lidar comparison in Brazil the difference for the trends at 50 km is outside the combined error estimates from the two datasets. Still, it is important to remember that the HALOE results are not specific to the longitude of the lidar measurements of Brazil.

Table 3 compares the trends from HALOE at three altitudes of the mesosphere with the values for previous decades from rocketsondes at 20N and 30N [*Keckhut et al.,* 1999] and from lidar at 44N [*Keckhut et al.,* 1995]. There is no significant difference for the trends from HALOE and the comparison datasets in the upper mesosphere (75 km), where $CO_2$ contributes the most to the effects of the radiative cooling. However, at 55 km the trends from HALOE are significantly smaller than those of the comparison techniques of the previous decades. *Akmaev et al.* [2006] reported globally-averaged trends in T(z) from their radiative model calculations that considered the changes due to $CO_2$ only (Case 1) and then those due to both $O_3$ and $CO_2$ (Case 2) for the period 1980-2000. Case 2 cooling trends (-1.5 to -2.0 K/decade) are about a factor of three greater than for Case 1 (-0.6 K/decade)—differences that qualitatively mimic the ones for 55 km between the comparison measurements of the earlier decade versus those of HALOE.

## 5. Summary Findings

The 14-yr HALOE dataset was obtained with a sampling frequency that is adequate for resolving the seasonal and longer-term variations of T(z) in the upper stratosphere and mesosphere, at least between the latitudes of about 40S to 40N. Though extending for just over one complete solar cycle, the HALOE T(z) time series yield 11-yr, max minus min temperature responses that are of order 1 K and in-phase with the solar cycle flux at low latitudes near the stratopause. Similar responses have been reported from ground-based lidar measurements and from model simulations. In the upper mesosphere the diagnosed, HALOE T(z) responses are somewhat larger at middle latitudes than from the models.

The cooling trends from the HALOE dataset are significant at most latitudes of the middle and lower mesosphere. They range from -1 K/decade at low latitudes to as much as -2.5 K/decade at the middle latitudes. Values of order -1 K/decade are reasonably consistent with those reported from lidar measurements at low latitudes and with those predicted for the radiative effects of the increasing $CO_2$. On the other hand, the cooling rates diagnosed from HALOE are generally larger than those from models for the upper mesosphere at the middle latitudes. The HALOE T(z) trends of the lower mesosphere are smaller than those published from rocketsondes and lidar measurements of the preceding two decades, presumably because those comparative results were obtained when the decreasing upper stratosphere ozone was an added factor for the total radiative cooling response through the lower mesosphere.

**Acknowledgments.** The author recognizes Prof. James Russell III (HALOE PI), the HALOE Science Team, and the many members of the HALOE Project Team at NASA Langley Research Center for their outstanding efforts over the years with regard to the operations of HALOE and in generating and characterizing the HALOE dataset. Initial findings for this study were presented at the 2007 EGU Meeting in Vienna, Austria. Results of the comparisons with the several station datasets were reported at the 2008 Fall AGU Meeting in San Francisco. The analyses were conducted with support from the UARS Project Office of the NASA Goddard Space Flight Center.

## References

Akmaev, R. A., V. I. Fomichev, and X. Zhu (2006), Impact of middle-atmospheric composition changes on greenhouse cooling in the upper atmosphere, *J. Atmos. Solar-Terr. Phys., 68*, 1879-1889.

Austin, J., et al. (2008), Coupled chemistry climate model simulations of the solar cycle in ozone and temperature, *J. Geophys. Res., 113*, D11306, doi:10.1029/2007JD009391.

Batista, P. P., B. R. Clemesha, and D. M. Simonich (2008), A fourteen year monthly climatology and trend in the 35-65 km altitude range from Rayleigh Lidar temperature measurements at a low latitude station, in press, *J. Atmos. Solar-Terr. Phys.,* doi:10.1016/j.jastp.2008.03.005.

Emmert, J. T., J. M. Picone, J. L. Lean, S. H. Knowles (2004), Global change in the thermosphere: compelling evidence of a secular decrease in density, *J. Geophys. Res., 109,* A02301, doi:10.1029/2003JA010176.

Gordley, L. L., E. Thompson, M. McHugh, E. Remsberg, J. Russell III, and B. Magill (2009), Accuracy of atmospheric trends inferred from the Halogen Occultation Experiment (HALOE) data, submitted to Journal of Applied Remote Sensing.

Hampson, J., P. Keckhut, A. Hauchecorne, and M. L. Chanin (2006), The effect of the 11-year solar-cycle on the temperature in the upper-stratosphere and mesosphere—Part III: investigations of zonal asymmetry, *J. Atmos. Solar-Terr. Phys., 68,* 1591-1599.

Hampson, J. P. Keckhut, A. Hauchecorne, and M. L. Chanin (2005), The effect of the 11-year solar-cycle on the temperature in the upper-stratosphere and mesosphere: Part II numerical simulations and the role of planetary waves, *J. Atmos. Solar-Terr. Phys., 67,* 948-958.

Keckhut, P., C. Cagnazzo, M.-L. Chanin, C. Claud, and A. Hauchecorne (2005), The effect of the 11-year solar-cycle on the temperature in the upper-stratosphere and mesosphere: Part I—assessment of observations, *J. Atmos. Solar-Terr. Phys., 67,* 940-947.

Keckhut, P., F. J. Schmidlin, A. Hauchecorne, and M. L. Chanin (1999), Stratospheric and mesospheric cooling trend estimates from U. S. rocketsondes at low latitude stations (8S-34N), taking into account instrumental changes and natural variability, *J. Atmos. Solar-Terr. Phys., 61,* 447-459.

Keckhut, P., A. Hauchecorne, and M. L. Chanin (1995), Midlatitude long-term variability of the middle atmosphere: trends and cyclic and episodic changes, *J. Geophys. Res., 100*, 18,887-18,897.

Laštovička, J., R. A. Akmaev, G. Beig, J. Bremer, and J. T. Emmert (2006), Global change in the upper atmosphere, *Science, 314*, 1253-1254.

Li, T., T. Leblanc, and I. S. McDermid (2008), Interannual variations of middle atmospheric temperature as measured by the JPL lidar at Mauna Loa Observatory, Hawaii (19.5N, 155.6W), *J. Geophys. Res., 113*, D14109, doi:10.1029/2007JD009764.

Matthes, K., U. Langematz, L. L. Gray, K. Kodera, and K. Labitzke (2004), Improved 11-year solar signal in the Freie Universtät Berlin Climate Middle Atmosphere Model (FUB-CMAM), *J. Geophys. Res., 109*, D06101, doi:10.1029/2003JD004012.

Remsberg, E. (2008a), On the observed changes in upper stratospheric and mesospheric temperatures from UARS HALOE, *Ann. Geophys., 26*, 1287-1297.

Remsberg, E. (2008b), On the response of Halogen Occultation Experiment (HALOE) stratospheric ozone and temperature to the 11-year solar cycle forcing, *J. Geophys. Res., 113,* D22304, doi:10.1029/2008JD010189.

Remsberg, E. (2007), A reanalysis for the seasonal and longer-period cycles and the trends in middle-atmosphere temperature from the Halogen Occultation Experiment, *J. Geophys. Res., 112,* D09118, doi:10.1029/2006JD007489.

Rind D., J. Lean, J. Lerner, P. Lonergan, and A. Leboissitier (2008), Exploring the stratospheric/tropospheric response to solar forcing, *J. Geophys. Res., 113,* D24103, doi:10.1029/2008JD010114.

Roble, R. G., and R. E. Dickinson (1992), How will changes in carbon dioxide and methane modify the mean structure of the mesosphere and thermosphere? *Geophys. Res. Lett., 16,* 1441-1444.

Russell III, J. M., et al. (1993), The halogen occultation experiment, *J. Geophys. Res., 98,* 10,777-10,797.

Shibata, K., and K. Kodera (2005), Simulation of radiative and dynamical responses of the middle atmosphere to the 11-year solar cycle, *J. Atmos. Solar-Terr. Phys., 67,* 125-143.

Sridharan, S., P. V. Prasanth, and Y. B. Kumar (2008), A report on long-term trends and variabilities in middle atmospheric temperature over Gadanki (13.5N, 79.2E), in press, *J. Atmos. Solar-Terr. Phys.*

Steinbrecht, W., et al. (2009), Ozone and temperature trends in the upper stratosphere at five stations of the Network for the Detection of Atmospheric Composition Change, in press, *Intl. J. of Remote Sensing.*

Tsutsui, J., K. Nishizawa, and F. Sassi (2009), Response of the middle atmosphere to the 11-year solar cycle simulated with the Whole Atmosphere Community Climate Model, *J. Geophys. Res., 114,* D02111, doi:10.1029/2008JD010316.

WMO (World Meteorological Organization) (2003), *Scientific assessment of ozone depletion: 2002*, Global Ozone Research and Monitoring Project, Report No. 47, 498 pp., Geneva.

**Figure 1.** Time series of bin-averaged sunrise (SR, open circles) and sunset (SS, solid circles) temperatures (in K) from Halogen Occultation Experiment (HALOE) measurements at 30±5N and 75 km altitude. Terms for the multiple linear regression (MLR) model fit are listed at the lower left (see text). The oscillating curve is the fit for the complete MLR model, while the straight line is the fit for just the constant plus linear trend terms.

**Figure 2.** Contour plot of the max minus min values of T(z) for the 11-yr term. Contour interval is 0.5 K, and the associated pressure profile (left) is approximate. Terms in regions with darker shading have confidence intervals (CI) of greater than 90%, while those of lighter shading have CI between 70 and 90%.

**Figure 3.** Phase of the maximum of the 11-year term (in years) as referenced to January 1991 or 2002. Contour interval is 1.5 years. Negative values are dashed, and the zero value is dotted. Terms in the shaded regions have a phase maxima within ±1.5 years of those two dates.

**Figure 4.** Contour plot of the adjusted, solar cycle (or SC-like) max minus min T(z) values. Contour interval is 0.5 K, and the zero and negative contours are dashed.

**Figure 5.** Contour plot of the linear trend terms for HALOE ozone versus pressure (%/decade). Contour interval is 2%. Negative trends have dashed contours, while the zero and positive trends are solid. Regions of darker shading have CI greater than 90%; lighter shading denotes CI of between 70 and 90%.

**Figure 6.** Contour plot of the diagnosed, linear trend terms for T(z) (in K/decade) from HALOE. Contour interval is 0.5 K/decade. Negative trends have the solid contours, while the zero and positive trends are dashed. Regions of darker shading have CI greater than 90%; lighter shading denotes CI of between 70 and 90%.

**Table 1**—Comparisons of Max-Min SC-like Responses for T(z) in deg K

| Altitude, km | | HALOE, 20±5N | Hawaii (19.5N), 94-07 | | HALOE, 10±5N | Gadanki (13.5N), 98-08 | | HALOE, 40±5N | OHP, (43.9N), 79-01 |
|---|---|---|---|---|---|---|---|---|---|
| 80 | | 1.9 | 0.0 | | 0.2 | --- | | 2.6 | 3.0 |
| 75 | | 1.5 | 0.2 | | 0.1 | -1.5 | | 2.9 | 2.3 |
| 70 | | 0.5 | -0.6 | | 0.4 | -1.5 | | 0.6 | 1.5 |
| 67 | | 0.1 | -0.4 | | 0.0 | -0.6 | | -0.1 | 2.2 |
| 64 | | 0.0 | 0.0 | | 1.0 | 0.0 | | 0.4 | 2.2 |
| 60 | | 0.6 | 0.5 | | 1.0 | 0.7 | | 1.4 | 2.2 |
| 53 | | 1.1 | 1.4 | | 0.5 | 0.4 | | 1.5 | 1.5 |
| 50 | | 0.6 | 0.4 | | 0.7 | 0.4 | | 1.0 | 0.5 |
| 47 | | 0.3 | 0.3 | | 0.9 | 0.3 | | 0.6 | 0.0 |
| 43 | | 0.4 | 1.3 | | 0.6 | 0.5 | | 0.4 | -2.0 |

**Table 2**—Comparisons of Concurrent Trends in T(z) in K/decade

| Altitude, km | | HALOE, 25±5S | Brazil, 23S, 93-06 | | HALOE, 10±5N | Gadanki, 13.5N, 98-08 |
|---|---|---|---|---|---|---|
| 60 | | -0.7 | -1.4 | | -1.2 | -1.9 |
| 53 | | -0.6 | --- | | -0.8 | -0.3 |
| 50 | | -1.0 | -2.3 | | -0.7 | -0.2 |
| 47 | | -0.5 | --- | | -0.2 | -0.5 |
| 43 | | -0.4 | --- | | -0.4 | 0.0 |
| 40 | | -0.7 | -1.1 | | | |

**Table 3**—Comparisons with Past Trends in T(z) in K/decade

| Altitude, km | | HALOE 20±5N | Rocketsonde 20N, 69-91 | | HALOE 30±5N | Rocketsonde 30N, 69-91 | | HALOE 45±5N | Lidar 44N, 79-93 |
|---|---|---|---|---|---|---|---|---|---|
| 75 | | -0.2 | -0.7 | | -2.2 | -2.9 | | -3.0 | -2.0 |
| 65 | | -1.5 | -2.8 | | -1.1 | -2.1 | | -3.5 | -3.0 |
| 55 | | -0.9 | -3.4 | | -0.6 | -2.7 | | -0.4 | -1.0 |

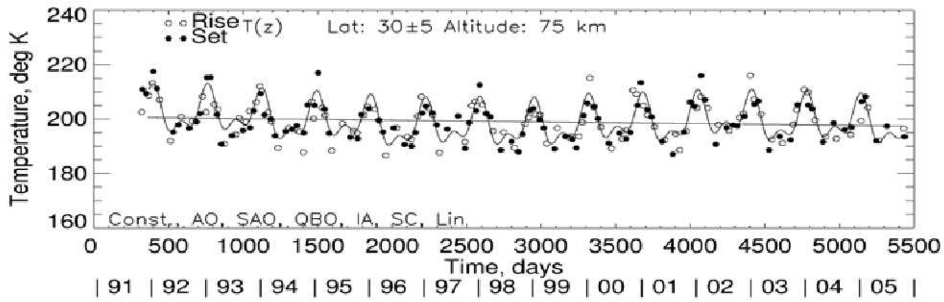


**Figure 1.** Time series of bin-averaged sunrise (SR, open circles) and sunset (SS, solid circles) temperatures (in K) from Halogen Occultation Experiment (HALOE) measurements at 30±5N and 75 km altitude. Terms for the multiple linear regression (MLR) model fit are listed at the lower left (see text). The oscillating curve is the fit for the complete MLR model, while the straight line is the fit for just the constant plus linear trend terms.

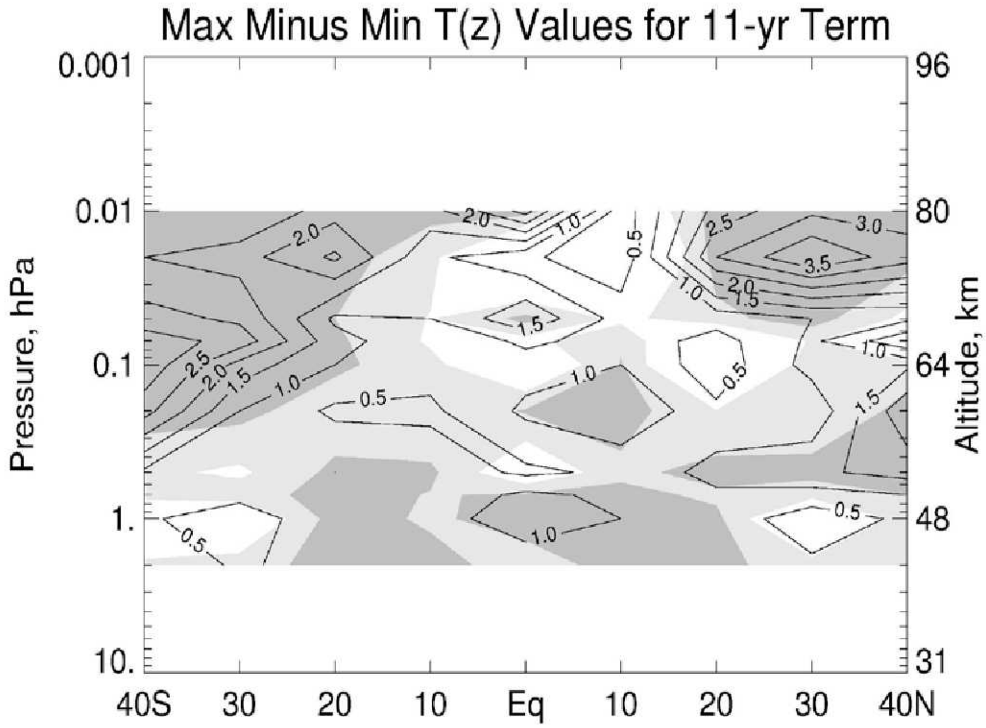


**Figure 2.** Contour plot of the max minus min values of T(z) for the 11-yr term. Contour interval is 0.5 K, and the associated pressure profile (left) is approximate. Terms in regions with darker shading have confidence intervals (CI) of greater than 90%, while those of lighter shading have CI between 70 and 90%.

402

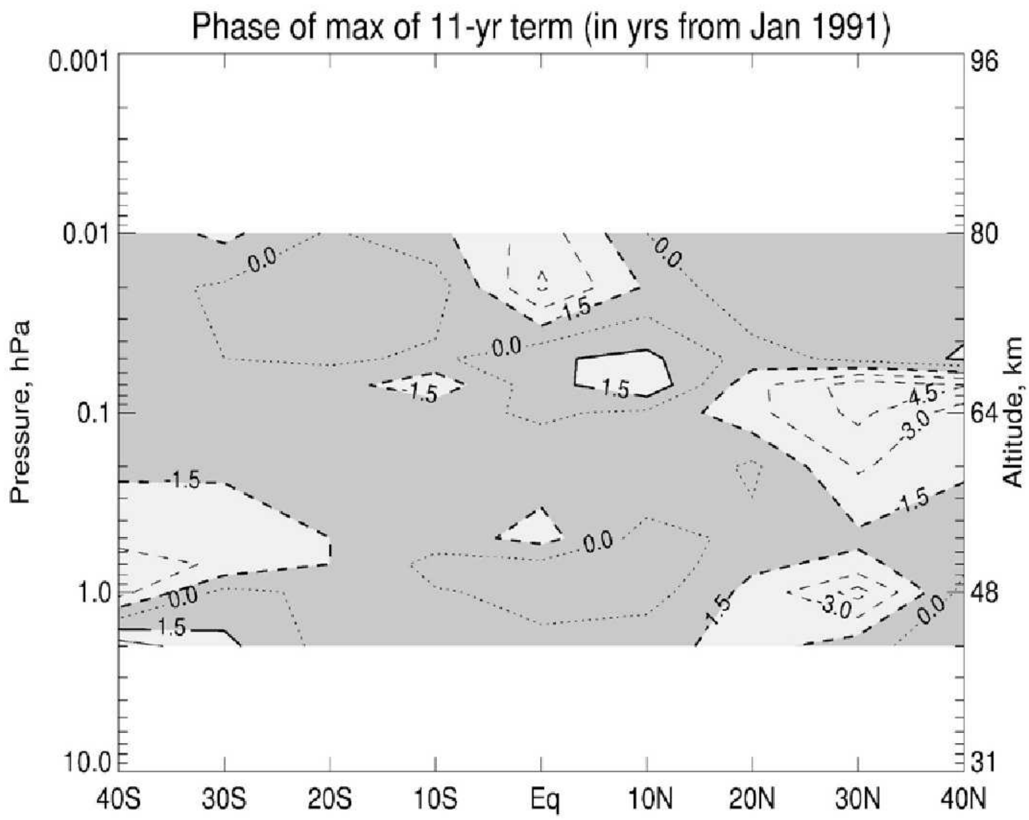


**Figure 3.** Phase of the maximum of the 11-year term (in years) as referenced to January 1991 or 2002. Contour interval is 1.5 years. Negative values are dashed, and the zero value is dotted. Terms in the shaded regions have a phase maxima within ±1.5 years of those two dates.

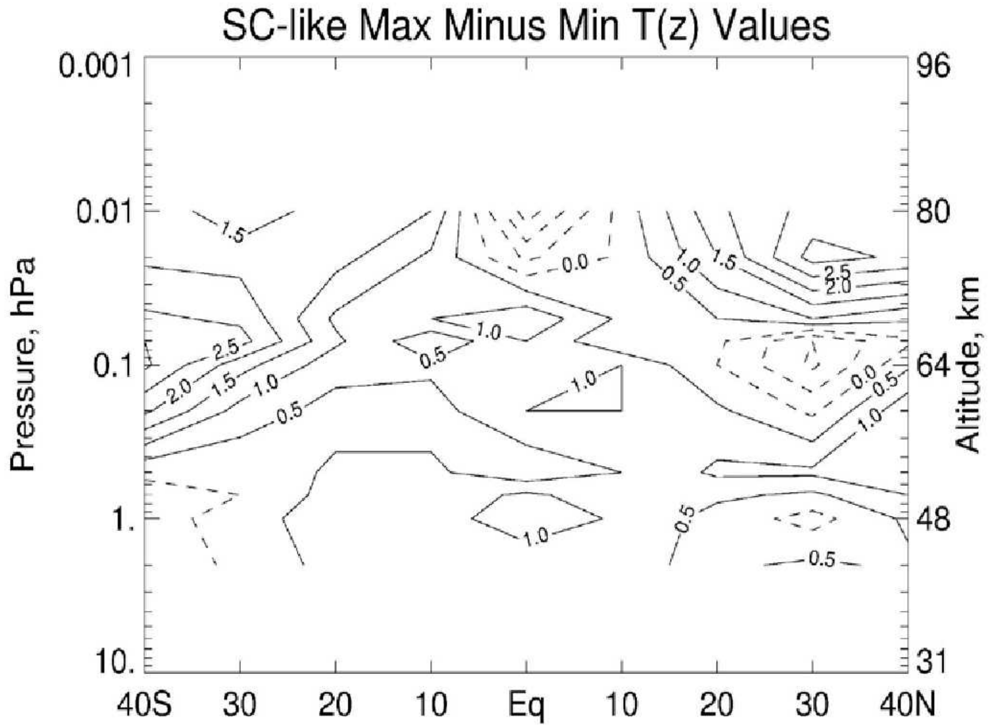


403 **Figure 4.** Contour plot of the adjusted, solar cycle (or SC-like) max minus min T(z) values. Contour interval is 0.5 K, and the zero and negative contours are dashed.

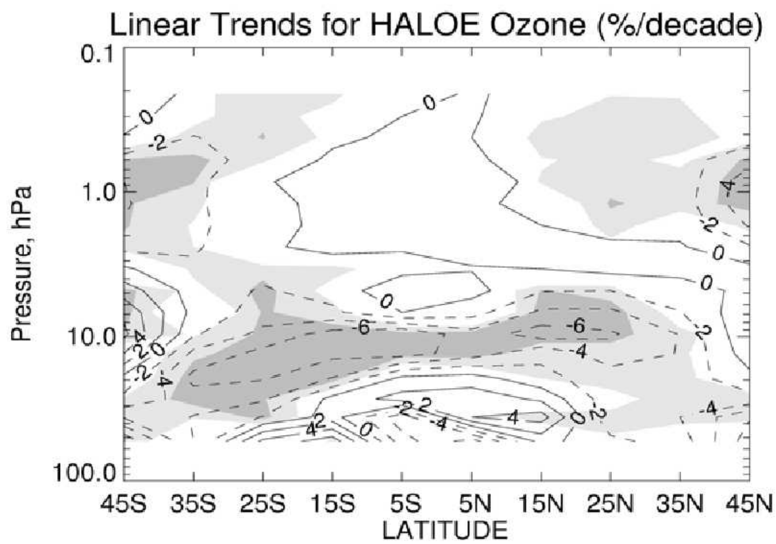


**Figure 5.** Contour plot of the linear trend terms for HALOE ozone versus pressure (%/decade). Contour interval is 2%. Negative trends have dashed contours, while the zero and positive trends are solid. Regions of darker shading have CI greater than 90%; lighter shading denotes CI of between 70 and 90%.

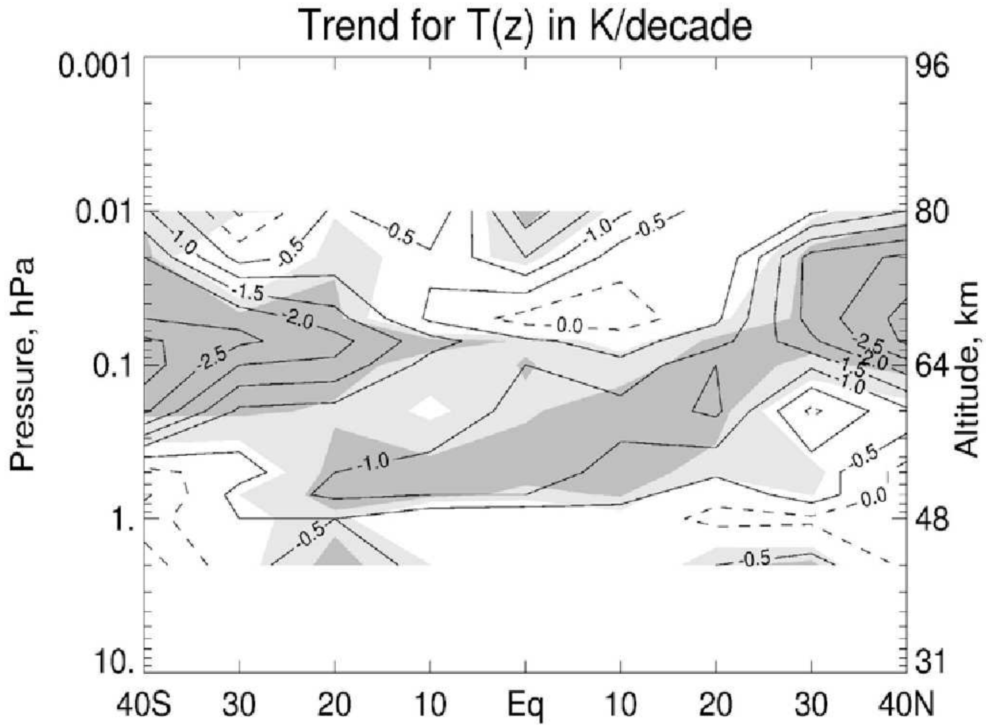


**Figure 6.** Contour plot of the diagnosed, linear trend terms for T(z) (in K/decade) from HALOE. Contour interval is 0.5 K/decade. Negative trends have the solid contours, while the zero and positive trends are dashed. Regions of darker shading have CI greater than 90%; lighter shading denotes CI of between 70 and 90%.